arXiv:cond-mat/0308438v2 [cond-mat.str-el] 20 Nov 2003

Fermi surface and quasiparticle dynamics of $Na_{0.7}CoO_2$ investigated by Angle-Resolved Photoemission Spectroscopy

M.Z. Hasan,[1, 2, 3] Y.-D. Chuang,[1, 3] A. Kuprin,[1, 3] Y. Kong,[1] D. Qian,[1] Y.W. Li,[1] B. Mesler,[3] Z. Hussain,[3] A.V. Fedorov,[3] R. Kimmerling,[3] E. Rotenberg,[3] K. Rossnagel,[3] H. Koh,[3] N.S. Rogado,[2, 4] M.L. Foo,[2, 4] and R.J. Cava[2, 4]

[1] *Joseph Henry Laboratories, Department of Physics, Princeton University, Princeton, NJ 08544*
[2] *Princeton Center for Complex Materials, Princeton Materials Institute (PMI), Princeton, NJ 08544*
[3] *Advanced Light Source, Lawrence Berkeley National Laboratory, Berkeley, Ca 94720*
[4] *Department of Chemistry, Princeton University, Princeton, NJ 08544*

(Dated: February 2, 2008)

We present an angle-resolved photoemission study of $Na_{0.7}CoO_2$, the host material of the superconducting $Na_xCoO_2 \cdot yH_2O$ series. Our results show a large hexagonal-like hole-type Fermi surface, a strongly renormalized quasiparticle band, a small Fermi velocity and a large Hubbard-U. Along the $\Gamma \rightarrow$M high symmetry line, the quasiparticle band crosses the Fermi level from M toward Γ consistent with a negative sign of effective single-particle hopping $\boldsymbol{t_{eff}}$ (estimated to be about 8±2 meV) which is on the order of exchange coupling $\boldsymbol{J}$ in this system. Quasiparticles are well defined only in the T-linear resistivity regime. Small single particle hopping and unconventional quasiparticle dynamics may have implications for understanding the unusual behavior of this new class of strongly correlated system.

PACS numbers: 71.20.-b, 74.90.+n, 73.20.At, 74.70.-b

Since the discovery of cuprate superconductivity [1], the search for other families of superconductors that might supplement what is known about the superconducting mechanism of doped Mott systems has been of great interest. The recent report of superconductivity near 5K in the triangular lattice, layered sodium cobalt oxyhydrate, $Na_{0.35}CoO_2 \cdot 1.3H_2O$, suggests that such materials may indeed be found [2]. The crystal structure of this material, and its precursor hosts, consists of electronically active triangular planes of edge sharing CoO_6 octahedra separated by Na (and hydration) layers that act as spacers, to yield electronic two-dimensionality, and also as charge reservoirs[2, 3, 4]. It has been argued that Na_xCoO_2 is probably the only system other than cuprates where a doped Mott insulator becomes a superconductor, although the fully undoped system has not yet been realized [5, 6]. $Na_{0.7}CoO_2$ is the host compound for these materials from which Na_x is varied to achieve superconductivity.

Despite some similarities with the cuprates, cobaltates show their own unique set of anomalous properties. For $Na_{0.7}CoO_2$ the anomalous Hall signal shows no saturation to 500 K [7], the thermopower is anomalously high and magnetic field dependent [8], there is linear-T resistivity (deviation from Fermi-liquid behavior) from 2 K to about 100 K [7] and there is strong topological frustration[5, 6, 9]. This class of systems may potentially contain new fundamental many-body physics and may as well be the realization of Anderson's original triangular lattice RVB system [10]. Therefore it is of interest to have a detailed look at the charge dynamics, starting with the host material. In this Letter, we report results of an angle-resolved photoemission (ARPES) study of $Na_{0.7}CoO_2$. A direct measurement of detailed Fermi surface topology and quasiparticle dynamics is of significant interest as it would provide a microscopic basis for understanding the complex electron behavior. We observe a large hole-type hexagonal-like Fermi surface. An extremely flat quasiparticle band is also found, which hardly disperses more than 75 meV. The quasiparticle weight decreases on raising the temperature to around 120 K and disappears where the T-linear behavior in resistivity disappears.

Single crystals of $Na_{0.7}CoO_2$ were grown by the flux method [7]. Measurements were performed at the Advanced Light Source Beamlines 12.0.1 and 7.0.2 using a Scienta analyzer. The data were collected with 30 eV or 90 eV photons with better than 30 meV energy resolution, and an angular resolution better than 1% of the Brillouin zone. The chamber pressure was better than 5×10^{-11} torr. Cleaving the samples in situ at 16 K resulted in shiny flat surfaces, characterized by optical (laser-reflection) and low-energy electron diffraction (LEED) methods to be flat, clean and well ordered with the same symmetry as the bulk. No signs of surface aging were seen for the duration of the experiments. Instead of cleaving several crystals to map the complete Fermi surface topology, we have worked on an image mode with fully motorized manipulator at BL7.0.2 ARPES endstation [11]. The entire Fermi surface topology could be mapped out within several hours after the cleavage.

Fig-1(a) shows the full valence band spectrum taken at 90 eV photon energy. It shows five prominent features: 0.7 eV, 3 eV (#2), 4.1 eV (#3), 6 eV (#4) and 11 eV (#5). The width of the main valence density of states being on the order of 7 eV is consistent with LDA calculations [12]. To account for the valence satellite one needs to consider the on-site Coulomb interaction (U) and clus-

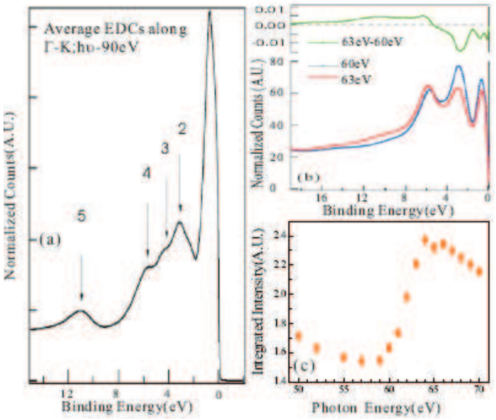

FIG. 1: Valence Excitations and Resonance Behavior :(a)Full valence band spectrum of $Na_{0.7}CoO_2$ taken at 90 eV photon energy. It shows five prominent features - the feature at 0.7 eV arises from Co t_{2g} states. (b) Valence band near Co:3p→3d resonant excitation (∼63 eV, red curve) compared with off-resonant excitation (∼60 eV, blue curve). Resonance behavior of valence excitations shows the enhancement of the 11 eV feature (green curve)- a correlation satellite. (c) Incident energy dependence of the 11 eV feature. It shows a Fano-type interference [15]

ter calculations provide a measure of U. Such calculations, with a strong Hubbard-U, suggest that the valence band has predominantly $^1A_1$ character (low-spin configuration $t_{2g}^x e_g^0$) and account for the 11 eV feature. We identify the 11 eV feature as a correlation satellite analogous to that seen in $LaCoO_3$[13], an indication of strongly correlated behavior with Hubbard-U ∼ 5 eV. The major low-energy feature is a broad band centered around 0.7 eV. Its resonance and photon-energy dependent behavior suggest that it consists of Co t_{2g} derived states, consistent with LDA and cluster calculations. Resonance behavior near $3p \rightarrow 3d$ excitation is shown in Fig.-1(b). Valence band near Co: $3p \rightarrow 3d$ resonant excitation (∼63 eV) is compared with off-resonant excitation (∼60 eV) by normalizing the area under both spectra to unity. Resonance behavior of valence excitations shows the enhancement of the broad 11 eV feature - a correlation satellite. Fig-1(c) shows the detail resonance behavior (Fano-type interference) of the correlation satellite. We also observe enhancements of the valence satellites under $2p \rightarrow 3d$ resonance (not shown here), supporting the identification of the 11 eV feature as a correlation satellite. Existence of such features and the resonance behavior are strong evidences for the system's highly correlated nature with large Hubbard-U similar to the cuprates [14, 15]. Further details of the resonance behavior would be reported elsewhere.

Much lower in energy near the Fermi level we observe a highly momentum (**k**-)dependent quasiparticle feature. Fig-2(a) shows this feature near the Fermi level crossing from M toward the Γ point in the Brillouin zone. Fig-2(b) shows part of the energy dispersion curves (EDCs) corresponding to Fig-2(a). This feature is well defined in momentum and energy and only weakly dispersive, hardly dispersing more than 80 meV. Beyond 75 meV the feature gets so broad (much broader than resolution) that the quasiparticle is not defined anymore in the sense that its lifetime is extremely short. To give a measure of bandwidth we first make a dispersion plot using the following procedure : take each EDC and subtract a background as shown in Fig.-2(c). Note that a step-like background is observed for all k as evident from Fig.-2(a). After background subtraction we take the centroid of the peak for its energy value (Fig.-2(c)). Based on these peak positions we make dispersion plots (Fig.-2(d) and (e)). To get a measure for bandwidth we extrapolate the band to the zone boundary as shown in Fig.-2(d) and (e). Since the band is narrow its extrapolation to the zone boundary is within the error bars of the measurement. This gives a value of about 70 ±10 meV. Just looking at the raw data (Fig.-2(a)) one could argue that the band is narrower than 100 meV. It is interesting to note that this band is not well defined over the full Brillouin zone - a case similar to the cuprates and other correlated systems (strong correlation can lead to significant lifetime shortening away from Fermi level). This can also be due to strong scattering by collective modes such as phonons [23]. A bandwidth of about 400-500 meV for cuprates is derived in a similar extrapolation basis [23]. Note that the cobaltate band is about at least a factor of 5 narrower than the cuprates.

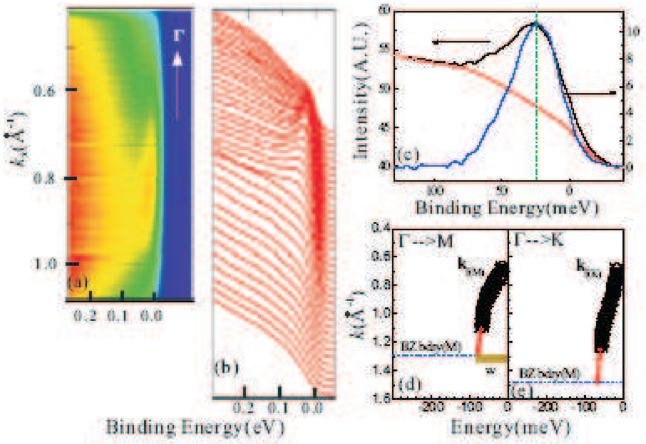

FIG. 2: Quasiparticle dispersion : (a)Γ →M Fermi crossing. Color red reflects the highest intensity - yellow to green to blue is in the order of decreasing intensity. (b) EDCs corresponding to the image plot in (a). (c) A single EDC for k = 0.78 $\AA^{-1}$. To extract the peak position a background is subtracted. A constant step-like background is best seen in Fig 2(a). Based on the extracted peak positions E vs. k plots are made and shown in (d) for Γ →M and in (e) for Γ →K directions.

Fig-3 shows the experimentally measured Fermi surface of $Na_{0.7}CoO_2$ over the complete Brillouin zone measured at a temperature of 16 K with a photon energy of 90 eV. The frequency-integrated spectral distribution, the n($\mathbf{k}$)-image, has been taken by integrating spectral weights within 75 meV below the Fermi level (and 25 meV above the Fermi level). It reveals a large hole-pocket centered around the Γ-point. The Fermi surface assumes a hexagonal character with an average radius of 0.7 ± 0.05Å^{-1}. This average is calculated based on half of the Brillouin zone measured(Fig-3 is symmetrized by two-fold). This is a bit larger than the size calculated for the related compound $NaCo_2O_4$ ($Na_{0.5}CoO_2$) using LDA [12]. If $Na_{0.0}$ corresponds to half filling, Luttinger theorem suggests hole pocket area of about 1/6 of the zone for the $Na_{0.7}$ case. The observed Fermi surface area is a bit larger under this scenario. It may indicate that a fraction of the doped electrons are in the Fermi sea, the rest are presumably localized and form local moments as seen in various experiments [7, 17, 18]. The shape of the Fermi surface in $Na_{0.7}CoO_2$ is rather hexagonal (anisotropic) in character in agreement with LDA [12]. We do not observe any of the small satellite pockets predicted by LDA calculations [12] around this large hexagonal Fermi surface (at least for the excitation photon energy of 90 eV where the search has been most extensive). This could be due to strong correlation effects, which can push the minority bands away from the Fermi level or wash out their relative intensity. It could also be due to the fact that one can not shift the chemical potential with doping in a trivial way as commonly observed in doped Mott systems so a straight forward rigid shift picture of the chemical potential for comparison may not be appropriate.

Along the $\Gamma \rightarrow$M Fermi crossing the quasiparticle band crosses the Fermi level from M toward Γ(Fig.2(a)) as opposed to Γ to M. Such a dispersion behavior is consistent with the negative sign of single-particle hopping ($\boldsymbol{t}$). Based on several EDC cuts we estimate the total bandwidth of this system which is about 70±10 meV (less than 100 meV). For a tight-binding hexagonal lattice total bandwidth $\boldsymbol{W} = 9\boldsymbol{t}$ where $\boldsymbol{t}$ is the nearest neighbor single-particle hopping. This gives a value of the effective single-particle hopping, $\boldsymbol{t}_{eff}$ of about 8±2 meV in this system [19]. It is interesting to note that this value is on the order of exchange coupling $\boldsymbol{J}$ ($\sim$ 10 meV)[17, 18] in this system. This bandwidth is an order of magnitude renormalization compared to mean field calculations, which suggest a bandwidth of order 1 eV to 1.4 eV[5, 6] or 0.48 eV[12]. Such enhancement of effective mass is in agreement with electronic specific heat measurements [20, 21]. Bandwidth suppression may also be responsible for enhancing the thermopower by an order of magnitude[8]. Single-particle hopping being on the order of exchange coupling suggests that the charge motion would be significantly affected by the spin dynamics of this system. Also a small value of $\boldsymbol{t}$ suggest that this system has an unusually small fermion degeneracy temperature compared to other metals.

Momentum distribution curves (MDCs) could be fitted with single Lorentzian function, on top of a linear background. The MDC fitting is known to produce reasonable results, especially when features are close to Fermi level E_f[22, 23] though not without controversies. Lorentzian lineshapes indicate that the quasiparticle self-energy is weakly dependent on the momentum normal to the Fermi surface [23]. We can then estimate the quasiparticle velocity normal to the Fermi surface. Such *MDC based* Fermi velocity is found to be less than 0.4 eV·Å. This value is much smaller than the nodal Fermi velocity of the cuprates ($\sim$ 1.5 eV·Å) extracted in a similar way. This is consistent with the fact that the cuprate bands are more dispersive [23]. We further studied the quasiparticle spectral weight near the Fermi level as a function of temperature (Fig.-4). The quasiparticle weight decreases to almost zero (background level) on raising the temperature to around 120 K (Fig.4(b)). This roughly coincides with the temperature where the T-linear behavior in resistivity gives way to stronger T-dependence (Fig.4(b)). Apparently, quasiparticles exist in this system only in the temperature regime where resistivity is linear in T and transport behavior is non-Fermiliquid like. This is in contrast with the conventional expectation that well defined quasiparticles are signatures of good Fermi liquid behavior. We also note that this temperature scale coincides with our scale of effective single-particle hopping $\boldsymbol{t}$ $\sim$ 8 meV $\sim$ 100 K. A dip is observed around 100 K in the temperature dependence of Hall coefficient[7]. This is also the temperature range when thermopower starts to deviate from linear-like behavior [7]. We argue that this is an important (and most relevant) energy scale to describe the physics of these systems. A strong lack of quasiparticle weight at higher temperatures is also reminiscent of the lack of quasiparticles in the high temperature normal state of cuprates [23]. But in cuprates, it is difficult to study the normal state over a large temper-

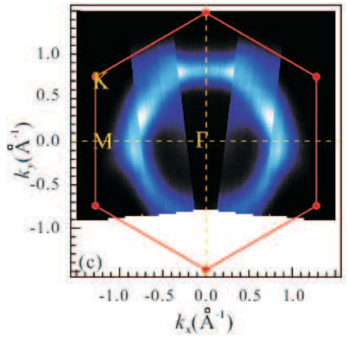

FIG. 3: Fermi surface : n(k) plot generated by integrating within 75 meV of Fermi level. A large hole-pocket is centered around the Γ-point. The Fermi surface, exhibiting some hexagonal anisotropy, is the inner edge of pocket as shown over the complete Brillouin zone.

ature range as it enters the superconducting state at a fairly high temperatures. Also cuprates can not be too heavily over doped. Cobaltates may offer the unique opportunity to study the normal state behavior of a heavily doped Mott system. This class of cobaltates has it's own uniqueness and hence interesting in its own rights. For the quasiparticle behavior, it may be that the transport in $Na_{0.7}CoO_2$ becomes incoherent well before a dimensional cross-over(two to three dimensional charge transport, [17]) is reached. Such behavior could be related to the highly frustrated nature of the antiferromagnetic interactions in a triangular lattice.

Previously studied layered cobaltates structurally similar to the cuprate family of $Bi_2Sr_2CaCu_2O_y$ such as $Bi_2Sr_{2.1}Co_2O_y$ and $Bi_{1.5}Pb_{0.5}Sr_{2.1}Co_2O_y$ were not reported to exhibit a quasiparticle state [24]. Cobaltates such as $(Bi_{0.5}Pb_{0.5})_2Ba_3Co_2O_y$ or $NaCo_2O_4$ exhibit quasiparticles and Fermi surfaces that were found to be roughly rounded, but an anisotropic shape was not reported [16]. In case of $Na_{0.7}CoO_2$ we find a hexagonal character and an even larger Fermi surface. The Fermi velocity in $Na_{0.7}CoO_2$ is found to exhibit anisotropy as much as 20%. A thorough comparison of $Na_{0.7}CoO_2$ with $Na_{0.5}CoO_2$ is difficult since detailed characterization of the latter has not been reported [16]. Unlike $Na_{0.5}CoO_2$, no dimensional crossover (two to three dimensional charge transport) exists in the $Na_{0.7}CoO_2$ up over to 300 K. The temperature dependence of quasiparticles look somewhat similar, however, hence we rather ascribe such temperature dependence in $Na_{0.7}CoO_2$ with the T-linear resistivity (non-Fermiliquid) regime. There are also dissimilarities at higher energies: the so called "broad hump" [16] around 0.7 eV is narrower and sharper (more than 500 meV) in $Na_{0.7}CoO_2$ than in $Na_{0.5}CoO_2$ for momentum(k) values near Fermi surface as seen in Fig.-4(b). Furthermore we see a strong temperature dependence of the 0.7 eV feature in $Na_{0.7}CoO_2$ - it tends to move toward higher binding energies at temperatures where the departure from a T-linear resistivity grows. The overall temperature induced spectral weight changes are found to be conserved within a range of 1 eV (changes in the valence band near the Fermi level due to changes in T occur only within 1 eV of the Fermi level). Such high sensitivity of temperature over a higher energy band (in addition to the quasiparticles) and large spectral weight redistribution is a further signature of this system's strongly correlated behavior [25] in addition to its highly flat band character which is typically the case for strong electron-electron correlation. A low temperature phase transition has been reported for $Na_{0.75}CoO_2$ -an indication that higher (commensurate) doping drives the system towards an ordering instability [26]. Despite the possibilities of kinematic nesting associated with the observed Fermi surface, the ordering in $Na_{0.75}CoO_2$ may be more complex due to the strongly correlated nature and the frustrated interactions in the system. But it would be interesting to study the nature of short-range dynamical correlations around q $\sim 3\pi/2$ using inelastic x-ray and neutron scattering techniques [27].

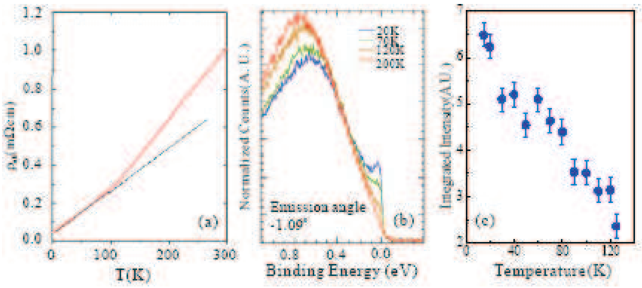

FIG. 4: Temperature Dependence : (a) In-plane resistivity in $Na_{0.7}CoO_2$ is linear up to 100 K [7] and then gradually crosses over to a stronger T-dependence. (b) Temperature dependence of quasiparticles near the $\Gamma \rightarrow$M Fermi crossing. The quasiparticle spectral weight ceases to exist above 120 K, close to the temperature where the T-linear behavior of the resistivity disappears. (c) Background subtracted integrated quasiparticle spectral weight is plotted as a function of temperature

In conclusion, we report an angle-resolved photoemission study of $Na_{0.7}CoO_2$. Resonant scattering of valence excitations indicate the existence of a large Hubbard-U supporting the strongly correlated nature of the system. The low-energy results reveal a large hexagonal-like hole-type Fermi surface and an extremely narrow quasiparticle band - an order of magnitude renormalization from the meanfield value. Such bandwidth suppression may be the key to understand the enhancements of thermopower and electronic specific heat. Effective single particle hopping being on the order of exchange coupling suggests that charge motion is significantly influenced by spin fluctuations in these systems. Effective (small) hopping being on the order of exchange coupling strongly indicates possible existence of unconventional physics (including RVB phases). Quasiparticles are well defined only in the T-linear resistivity (non-Fermi liquid) regime. From a theoretical perspective, it would be interesting to understand the emergence of this small degenerate energy scale in the cobaltates. The system's strongly correlated nature as manifested from this extremely narrow band and large spin-entropy observed by transport measurements [7] taken together may shed clues to understand the broad spectrum of unusual properties including superconductivity at low doping. It would be interesting to study the doping evolution of the Fermi surface and quasiparticle behavior of these systems by combining ARPES and newly developed momentum resolved inelastic x-ray scattering [27]. Furthermore, any comprehensive theory for cobaltates need to account for the low degenerate energy scale and unconventional quasiparticle dynamics observed.

The authors thank P.W. Anderson, N.P. Ong, P.A.

Lee, D.A. Huse, P.M. Chaikin, A. Millis, S. Sondhi, J. Lynn, S. Maekawa, A. Vishwanath and Y. Wang for valuable discussions. The experiment was performed at the ALS of LBNL, which is operated by the U.S. DOE's BES with contract DE-AC03- 76SF00098. MZH acknowledges partial support through NSF-MRSEC (DMR-0213706) grant and R.H. Dicke Award by Princeton Univ. Materials synthesis supported by DMR-0213706 and the DOE, grant DE-FG02-98-ER45706. Email correspondence : mzhasan@Princeton.edu

[1] J.G. Bednorz and K.A. Muller, Z. Phys.B 64, 189 (1986).
[2] K. Takada et.al., Nature 422, 53 (2003).
[3] M.L. Foo et.al., Solid State Comm. 127, 33 (2003).
[4] R. Schaak et.al., Nature 424, 527 (2003).
[5] G. Baskaran cond-mat/0303649.
[6] Q. Wang, D.H. Lee and P.A. Lee cond-mat/0304377.
[7] Y. Wang et.al., Nature 423, 425 (2003); Y. Wang et.al., cond-mat/0305455.
[8] I. Terasaki et.al., Phys. Rev. B 56, R12685 (1997).
[9] B. Kumar and B.S. Shastry, cond-mat/0304210.
[10] P.W. Anderson, Mat. Res. Bull., 8, 153 (1973); P.W. Anderson, Science 235, 1996 (1987).
[11] E. Rotenberg et.al., Nature 406, 602 (2000).
[12] D.J. Singh Phys. Rev. B 61, 13397 (2000).
[13] T. Saitoh et.al., Phys. Rev. B 55, 4257 (1997).
[14] A.J. Arko et.al., Phys. Rev. B 40, 2268 (1989).
[15] Z.X. Shen and D. Dessau, Phys. Rep., 253, 53 (1995).
[16] T. Valla et.al., Nature 417, 627 (2002).
[17] Y. Wang et.al., (unpublished).
[18] R. Ray et.al., Phys. Rev. B 59, 9454 (1999).
[19] It would also be interesting to consider the effect of Kagome interactions (W. Koshibae and S. Maekawa cond-mat/0306696) rather than the hexagonal structure in estimating the effective hopping which will make it a bit larger but still keeps the value on the order of about 10 meV.
[20] Y. Ando et.al.,Phys. Rev. B 60, 10580 (1999).
[21] M. Bruhwiler et.al., cond-mat/030931.
[22] Y.-D. Chuang et.al., Science 292, 1509(2001).
[23] A. Damascelli et.al., Rev. Mod. Phys. 75, 473 (2003).
[24] T. Mizokawa et.al., Phys. Rev. B 64, 115104 (2002).
[25] C. Kim et.al., Phys. Rev. B 65, 174516 (2002).
[26] T. Motohashi et.al., Phys. Rev. B 67, 064406 (2003).
[27] M.Z. Hasan et.al., Science 288, 1811 (2000) and Phys. Rev. Lett. 88, 177403 (2002).